

Characterization and FEM-based Performance Analysis of a Tonpiliz Transducer for Underwater Acoustic Signaling Applications

*Venkatesh Vadde and Bhagya Lakshmi G.

ECE Department, PES Institute of Technology

*Corresponding author: PESIT, 100-Foot Ring Road, BSK-III Stage, Bangalore-85; vvadde@gmail.com

Abstract: Underwater acoustic signals need transducers to generate and detect signals with high power, linearity, dynamic-range and beam-width. Among a variety of transducer designs, a Tonpiliz transducer stands out for power and long-range applications. A Tonpiliz transducer for underwater acoustic signaling is developed to scale and analyzed using FEM tools with Comsol. The underlying pressure-acoustics and piezoelectric phenomena are examined as a function of sizing, transducer dimensioning, materials, and variability. Using FEM tools, we analyze and evaluate key transducer performance specs such as resonant frequency, tunability, material-choices, beam-pattern and scalability. Using Comsol as a design tool, one can develop low-cost, reliable, miniature transducers for sonar signaling and ultrasonic scanners.

Keywords: Underwater acoustics, Tonpiliz transducer, ultrasonic, hydrophone design.

1. Introduction

Underwater communication and sonar signaling in naval systems is routinely based on acoustic instead of electromagnetic signals. These acoustic signals, spanning a 10Hz-40KHz frequency range, propagate much better and farther in underwater channels, suffering lesser attenuation at lower frequencies. The propagation of acoustic signals itself is well understood and widely used in naval system design. However, in underwater acoustics, our sonar-signaling ability for communication and ranging is limited mostly by the transducers. It is rather challenging to design underwater transducers at the most usable frequencies, and as such the design of efficient acoustic projectors or receivers is a subject of great interest.

A very good exposition of the design of underwater acoustic transducers can be found in [1]. Several attempts have been made to model, design and study the performance of underwater transducers [2-5]. The key parameters that have been explored to study transducer performance

include head-sizing and shape [2], the influence of an air-gap in the transducer [3], relative thickness of the transducer head-mass and tail-mass along with angle of taper of the cone [4]. In [5], the authors explore miniaturization of the transducer, which finds applications in array development. Material science of the Piezo-ceramic stack has been the subject of some research [6], with optimization based on statistical regression analysis [7-8].

In this paper, we develop and analyze a standard piezoacoustic Tonpiliz-transducer model for underwater acoustics in Comsol by addressing the attendant piezoelectric and pressure acoustic multiphysics phenomena. Transducer properties that are studied and characterized are the center frequency, bandwidth, linearity, scaling, and beam-pattern.

2. Tonpiliz Transducer Design

The Tonpiliz (German for “sound mushroom”) transducer consists of an acoustically active ceramic stack, sandwiched between a head and tail piece. Since the specific impedance of the ceramic is higher than that of water, a better impedance match would be achieved if the area of the radiating face is significantly larger than that of the piezoelectric materials. This concept along with a tail mass allows a compact means for obtaining high output at midrange frequencies without the need for an excessively long piezoelectric ceramic drive stack.

The material used in the head-piece is chosen to have an acoustic impedance between that of the ceramic and water. The tail section has the highest impedance. This is so that the overall transducer will act like a piston with most of the displacement occurring at the head-piece. The tail-piece usually radiates into air, so the large impedance mismatch helps to reflect energy back to the head section, improving its radiating performance. The whole structure is placed

under compressive pre-stress by placing a bolt through the middle.

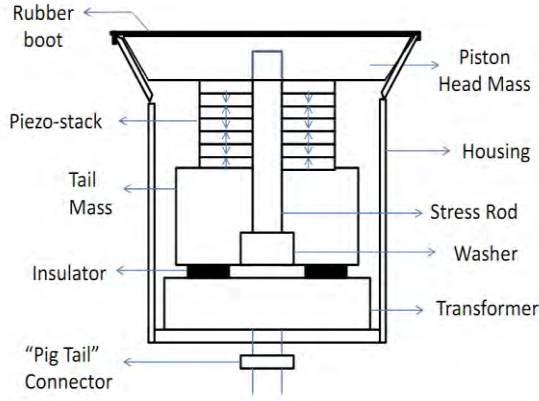


Fig.1. Cross-section of Tonpiliz transducer

A cross section of a typical Tonpiliz transducer is illustrated in Fig.1 above with a 33-mode driven ring stack of eight parallel wired PZT rings. The piezo-stack drives a relatively light but stiff piston mass with a comparatively heavy tail-mass at the other end. The assembly also includes mechanical isolation elements, a housing, transformer with tuning network, rubber enclosure around the head, and electrical underwater connector.

The Tonpiliz transducer designed and modelled by us employs an alumina head, typically, with tail of steel (or copper), and a BeCu-alloy stress rod. The piezoelectric stack consists of PZT4 (lead zirconate titanate) ceramic rings. The table below gives information on the material characteristics and size of transducer parts used for 2D axis-symmetric FEM analysis:

Material employed	Density (kg/m ³)	Sound speed (m/s)
Alumina	3690	9020
Copper	8800	3901
Steel	7900	4940
Be-Cu alloy	8200	3900
PZT4	7550	2930
Water	1000	1500

Table-1: material properties of transducer parts

Width (mm)	Height (mm)	Part of the Transducer
30	8.4	Head-mass
17	39.6	Tail-mass
1.5	14	Stress rod
14	12	Drive stack

Table-2: dimensions of the transducer

The total size of transducer without miniaturization is 60mm*60mm. It is generally preferred to operate the transducer close to resonance not just for high transducer gain, but also to avoid harmonic distortions which tend to be higher away from resonance.

2.1 Transducer Piezoelectric Basics

The performance of the transducer is governed by the physics of piezoelectricity, which helps to convert electrical signals to mechanical vibrations. The piezoelectric effect can be described in terms of the 2nd rank stress tensors in the form of stress vector T and strain vector S , and their relation to the electric field, E and electric displacement, D . The phenomenon of piezoelectricity can then be quantified through the following equations:

$$S = s^E T + d^t E \quad \text{Eq. (1a)}$$

$$D = d T + \epsilon^T E \quad \text{Eq. (1b)}$$

Here, S and T are 6x1 column vectors, E and D are 3x1 column vectors, s^E is a 6x6 matrix of elastic compliance coefficients, d is a 6x3 matrix of piezoelectric coefficients. For piezoelectric crystals of class C_{6v} , and for permanently polarized electrostrictive materials, many of the coefficients are zero and others are related, leaving only 10 independent coefficients. Thus, we have the following relationships:

$$\begin{aligned} S_1 &= s_{11}^E T_1 + s_{12}^E T_2 + s_{13}^E T_3 + d_{31} E_3, \\ S_2 &= s_{12}^E T_1 + s_{11}^E T_2 + s_{13}^E T_3 + d_{32} E_3, \\ S_3 &= s_{13}^E T_1 + s_{13}^E T_2 + s_{33}^E T_3 + d_{33} E_3, \\ S_4 &= s_{44}^E T_4 + d_{24} E_2, \\ S_5 &= s_{44}^E T_5 + d_{15} E_1, \\ S_6 &= s_{66}^E T_6, \\ D_1 &= d_{15} T_5 + \epsilon_{11}^T E_1, \\ D_2 &= d_{24} T_4 + \epsilon_{22}^T E_2, \\ D_3 &= d_{31} T_1 + d_{32} T_2 + d_{33} T_3 + \epsilon_{33}^T E_3 \end{aligned} \quad \text{Eq.(2a-2i)}$$

where $s_{66}^E = 2(s_{11}^E - s_{12}^E)$ and the subscripts 4, 5, 6 refer to shear stresses and strains.

For a Tonpiliz transducer operated in the 33-mode, where the displacement through tail is negligible, T_1, T_2, T_4, T_5 play an insignificant role, and the equations reduce to the following:

$$\begin{aligned} S_1 &= s_{13}^E T_3 + d_{33} E_3, \\ S_2 &= s_{13}^E T_3 + d_{32} E_3, \\ S_3 &= s_{33}^E T_3 + d_{33} E_3 \\ D_3 &= d_{33} T_3 + \epsilon_{33}^T E_3 \end{aligned} \quad \text{Eq. (3a-3d)}$$

Note that, in this case, it is convenient to make stress an independent variable, because the unimportant strains, S_1 and S_2 , are then analytically separated from the important strain, S_3 . Thus S_3 and D_3 are the main parameters of interest which is solved in FEM tool COMSOL.

Eqns (3c-3d) provide the basis for the two transducer equations. If the Piezo is short enough, the displacement varies linearly along its length from zero at the fixed end to a maximum at the end attached to the Head. The stress and strain, T_3 and S_3 , are then constant along the length, and the force exerted on the mass by the bar is $A_0 T_3$.

2.2 Transducer Equivalent Circuit

A simplified lumped model may be used as an aid in understanding and implementing an initial design. Normally, this model would be followed by more accurate distributed and finite element models. The lumped mode representation is a reasonably good model for a Tonpiliz Transducer as the size and shape of respective parts favour such a reduction to lumped masses and spring. Consequently mass of the drive section M_s , should be included and distributed along with the Head mass M_h , and tail mass M_t , in even the simplest lumped models.

A lumped mechanical model of the Tonpiliz transducer with minimum essential parts is illustrated in Fig.2 and may be used as a basis for the equivalent circuit of Fig.3. It is worth noting that the transducer design itself aims to optimize the mechanical model. The electrical equivalent circuit helps us in electrical tuning, analysis and impedance matching of the transducer so that we can optimally drive the device.

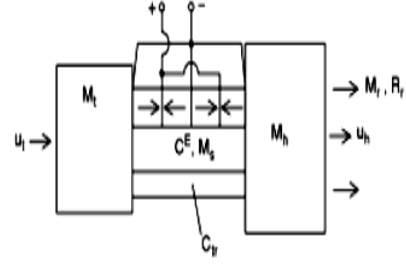


Fig.2 Basic Mechanical lumped model

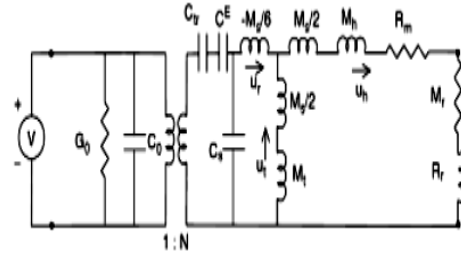


Fig.3. Lumped equivalent circuit of a Tonpiliz transducer

The circuit parameters are

$$\begin{aligned} G_0 &= \omega C_f \tan \delta, \\ C_f &= n \epsilon_{33}^T A_0 / t, \\ C_0 &= C_f (1 - k_{33}^2), \\ N &= d_{33} A_0 / t_{33}^E, \\ C^E &= n t s_{33}^E / A_0 \end{aligned} \quad \text{Eq (4a-4e)}$$

where $R_0 = 1/G_0$, n is the number of rings in the drive stack, t is the thickness of each ring, C^E is the short circuit compliance of the drive stack, C_{tr} is the compliance of the stress rod assembly, R_m is the mechanical loss resistance, R_r is the radiation resistance, M_r is the radiation mass, u_h is the velocity of the head, u_t is the velocity of the tail, and the relative velocity between the two is $u_r = u_h - u_t$. As the stack expands the head and tail move in opposite directions. The head mass, tail mass and relative velocity magnitudes are inter-related [1].

A large tail-to-head mass is desirable as it yields a large head velocity, radiating the most power. If $M_h = M_t$ then $|u_h| = |u_t|$ and $u_h = u_t/2$ which is 6 db less in source level than if $u_t = 0$, which is approached if $M_t \gg M_h$. Typical Tonpiliz designs use tail to head mass ratio range from 2 to 4 as larger values lead to too much weight. In our design the ratio has been maintained as 3. A design with a low-mass piston head allows a

large M_t/M_h ratio without as much weight burden. The first flexural resonance of the head should be significantly above the operating band.

The design of the tail mass is the simplest task. The tail is usually less than a quarter-wavelength long with a diameter slightly greater than the diameter of the driving stack. It is typically in the form of a Copper cylinder, solid steel cylinder, occasionally of tungsten in smaller higher frequency designs, with a hole through the centre to accommodate the stress rod. The stress rod exerts a compressive stress T_0 on the ceramic to prevent the drive stack from operation in tension under high drive conditions. The corresponding tensile stress in the stress rod of cross-sectional area A_t is $T_t = T_0 A_0 / A_t$. Because of the typically large area ratio, the stress rod must be made of high strength steel, Beryllium copper UNS C17200, or titanium. The stiffness of the stress rod is usually made about 10% or less of the drive stack stiffness to prevent significant reduction in effective coupling coefficient.

3. Simulation Results & Discussion

A model of the Tonpiliz transducer to scale was built using Comsol for simulation. The accompanying multiphysics phenomena encompass pressure-acoustics and piezo-acoustics. The 6cmx6cm transducer has an alumina head, a stack of piezo-ceramic discs made of PZT4, and a tail of steel. The pre-stress rod joining the piezo-ceramics to the head was chosen to be made from the Be-Cu alloy. The transducer was designed to be axisymmetric, and the head-mass was interfaced to a semi-infinite body of water. The piezo-stack is then driven using a CW-signal at or close to the resonant frequency.

Since our objective here is to primarily study the Tonpiliz transducer as a sound projector, we measure the transducer performance in terms of the sound-pressure level (SPL) along a circular arc of 1m-radius away from the transducer's body. We have studied the transducer frequency response, power-vs-voltage response, tunability, beam-pattern and its response when scaled in size.

We depict in Fig.4, the transducer response to various signal drive levels, wherein the acoustic

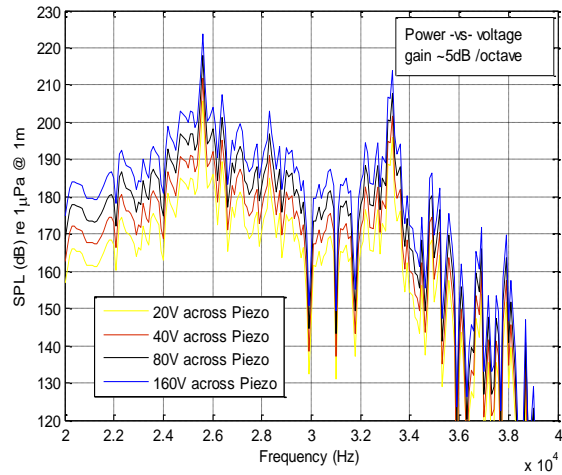


Fig.4. Sound pressure level versus frequency for various drive-signal levels

RMS pressure level is measured relative to $1\mu\text{Pa}$. We find that the transducer exhibits a power differential of 5dB per octave, which is quite appreciable given the size of the transducer. In Fig.4, we can also clearly see that the transducer exhibits primary resonance around 25.5KHz, and then a secondary resonant peak at about 33KHz. Our goal was to test an experimental transducer whose resonance is observed around 24.5KHz, and there is reasonable agreement from simulation results.

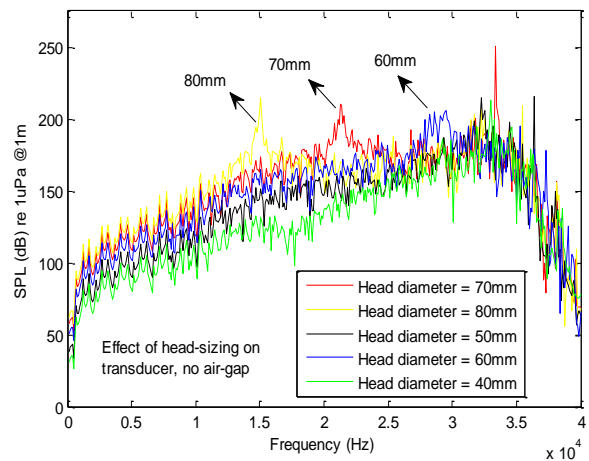


Fig.5. Tuning the transducer response using head-size and dimension

One of the key parameters that can influence the resonant frequency response is the head-size,

and its proportion to the tail-mass. In our simulations, we kept the tail-mass fixed, and varied the head diameter from 40mm to 80mm, the default sizing being 60mm.

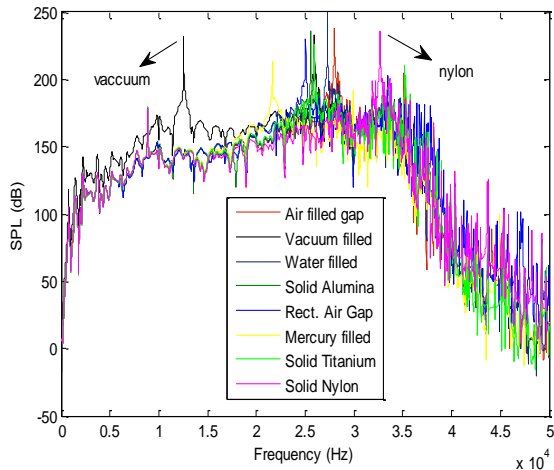


Fig.6. Effect of head-mass and head-material on the transducer frequency response

Similarly, frequency response can be tuned by using a different material for the head-mass as well as by creating an air-gap in the head. The effect of head-mass for various material candidates, as well as of an air-gap is illustrated in Fig.6. The resonant frequency is smallest when we use a hermetically sealed gap, and can be as large as 32.5KHz for a nylon head. The nylon-head case is interesting since it can find many uses in low-power applications and is easy to fabricate. It is evident that with a combination of sizing and material choice we can considerably tune the resonant frequency.

For a transducer, it is of considerable interest to examine its beam-pattern. We simulated the beam pattern for a transducer with and without an air-gap. The beam patterns are shown in Fig.7. It is interesting to note that the transducer with an air-gap has no broad side-lobes in the 30°-60° range, whereas the solid-head transducer has broader side-lobes. The transducer with an air-gap also seems to have a more directional pattern along boresight. Overall, we could say that the transducer is more directional when having an air-gap.

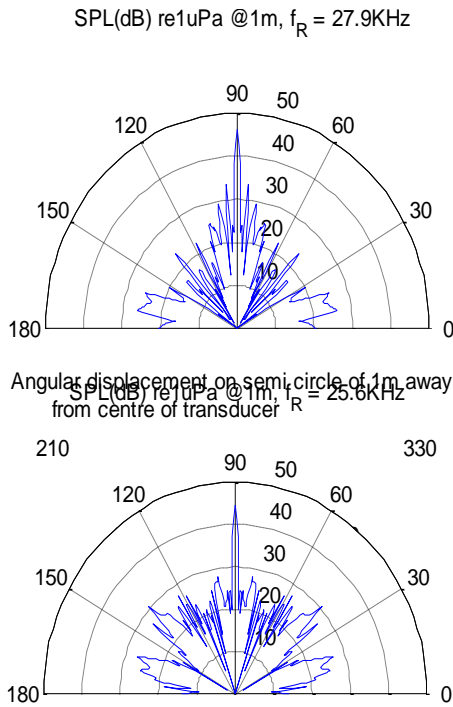


Fig.7. Beam pattern for a transducer with an air-gap and without an air-gap @ 1m away from the centre of transducer

The transducer performance for various head-sizes is shown in Fig.5. We note that as the head-size increases, the f_R shifts downwards.

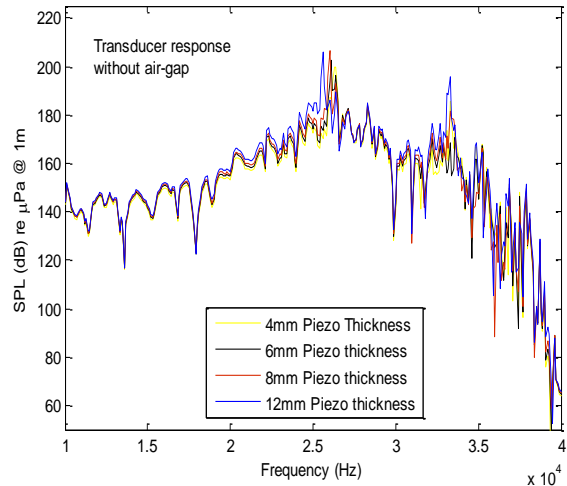


Fig.8. Effect of piezo-ceramic stack thickness on the transducer response

In another study, we varied the piezo-stack thickness as shown in Fig.8, and we find that the transducer response alters very slightly. In other words, the piezo-disc thickness has no role to play in tuning frequency response.

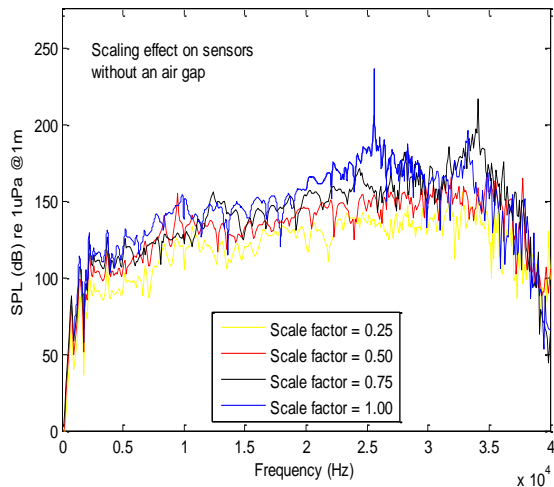


Fig.9. Transducer frequency response for various scale-factors.

Lastly, we examined transducer performance under miniaturization. It appears, from Fig.9, that mechanical effect of scaling is to slightly shift the transducer resonant frequency slightly to the right. The ability to make small transducers with reasonable power levels will enable us to build transducer arrays with vector sensing capabilities.

4. Conclusions

We successfully developed and analyzed a Tonpilz transducer for underwater acoustics in Comsol. The head design plays an important role in characterizing the performance of a transducer. The head-mass, material and diameter was seen to be a key determinant of the resonant frequency. We found the directional properties of a transducer with an air-gap to be better than without an air-gap. The transducer properties are fairly constant upon miniaturization. Using Comsol, it is possible also to do a study on performance variability, which can be useful in developing uniform and identical transducers.

5. Acknowledgements

We gratefully acknowledge support from the Naval Research Board-India under grant number DNRD/05/4003/NRB/183, and also a University grant, VTU/Aca/2009-10/A9/11625 which together helped us carry out this research.

6. References

- [1] C.H. Sherman and J.L. Butler "Transducers and arrays for underwater sound" Springer, New York (2006)
- [2] D.W. Hawkins, P.T.Gough "Multiresonance design of a Tonpilz transducer using the FEM method", IEEE Trans. on UFFC, **Vol. 43**, No. 5, (1986)
- [3] S. Chhith, Y. Roh "Wideband Tonpilz transducer with a cavity inside a head mass", Jap. Jnl. of Applied Physics, **Vol. 49** (2010)
- [4] Q. Yao and Leif Bjorno, "Broadband Tonpilz underwater acoustic transducers based on multimode optimization" IEEE Trans. UFFC, **Vol. 44**, no. 5 (1997)
- [5] Y. Roh and X. Lu "Design of an underwater Tonpilz transducer with 2-2 mode piezo-composite materials" Proc. ASA Mtng, pp. 3734-3740 (2006)
- [6] K. Kang, Y. Roh, "Optimization of structural variables of a flexensional transducer by the statistical multiple regression analysis method" Proc. ASA Mtng, (2003)
- [7] T. Inoue, M. Yamamoto, *et al*, "An investigation for miniaturised, light-weight and high-power Tonpilz piezoelectric transducers" ICICE Trans. Electron., **Vol E83-C**, no. 3 (2000)
- [8] Y-C. Chen, Sean Wu, *et al*, "Lump circuit modeling and matching consideration on acoustical transmitters for underwater application" Jnl. of Marine Sci. and Tech., **Vol. 12**, No. 3, pp. 152-158 (2004)
- [9] S.C. Thompson, R.J. Meyer and D.C. Markley, "Coupling coefficient of segmented stack piezoelectric transducers using high-coupling materials," J. Acoust. Soc. Am., **Vol.124**, pp. 2487 (2008)